Synthesis and Characterisation of Cyanide-bridged Heterobinuclear Mixed-valence Compounds based on Cyclopentadienylorganophosphine-ruthenium(II) and -osmium(II) Cyano and Pentaammine-ruthenium(III) and -osmium(III) Moieties

William M. Laidlaw and Robert G. Denning*
Inorganic Chemistry Laboratory, University of Oxford, South Parks Road, Oxford OX1 3QR, UK

Six novel cyanide-bridged mixed-valence complexes, $[(\eta^5\text{-}C_5H_5)(PPh_3)_2M'(\mu\text{-}CN)M(NH_3)_5][CF_3SO_3]_3$ (M = Ru, M' = Ru or Os; M = Os, M' = Ru or Os) and $[(\eta^5\text{-}C_5R_5)(PPh_3)_2Ru(\mu\text{-}CN)Ru(NH_3)_5][CF_3SO_3]_3$ (C_5R_5 = C_5H_4Me or C_5Me_5), have been synthesised using a simple coupling reaction and characterised by electronic and infrared absorption spectroscopy and by cyclic voltammetry. They exhibit moderately intense ($\varepsilon_{max} \approx 2000$–$4000$ dm^3 mol^{-1} cm^{-1}), broad ($\Delta\nu_{\frac{1}{2}} \approx 5000$ cm^{-1}) intervalence charge-transfer transitions in the visible spectrum, analysis of which reveals Robin–Day Class II behaviour ($\alpha^2 \approx 0.8$–2.0%, $H_{rp} \approx 1700$–2000 cm^{-1}). Outer-sphere effects upon the cyanide-bridge stretching frequency and all the intervalence charge-transfer band characteristics are reported and interpreted using linear correlations with respect to Gutmann solvent donicity, where appropriate, and simple perturbation arguments. The weak solvent dependence of the coupling element, H_{rp}, indicates that the charge-transfer mechanism proceeds primarily through an electron, rather than hole, transfer pathway. The intervalence charge-transfer bands of the cyclopentadienylosmium complexes exhibit a pronounced spin-orbit splitting, the relative intensities of the components also showing solvent dependence.

Intervalence charge-transfer (i.v.c.t.) transitions, characteristic of discrete mixed-valence compounds of the form $[L_DD(\mu\text{-}X)AL_A]$ comprising donor, D, and acceptor, A, metals, ligand environments, $L_{D,A}$, and an intermetallic bridge, X, have been widely studied to probe kinetic and thermodynamic effects of fundamental interest to the field of electron transfer.[1–3] The electronic properties[4] of such systems depend critically upon the nature of the metals, ligands, bridge and even solvent,[5,6] and form the basis of the widely recognised Robin–Day classification scheme.[7]

We[8,9] have undertaken a systematic programme to synthesise novel cyanide-bridged Class II mixed-valence compounds to enable the study of their non-linear optical,[10–12] spectroscopic and redox properties. In this report, we use cyclopentadienylorganophosphinemetal(II) donor and pentaamminemetal(III) acceptor groups to combine the features of both organometallic[9,13] and classical[8,14] ligand-based cyanide-bridged systems, discussing their synthesis and their electrochemical, infrared and intervalence absorption characteristics.

As background, we briefly recall the Hush formalism[15] for describing intervalence electron transfer. If the wavefunctions ψ_r and ψ_p describe the fully localised oxidation-state redox isomer configurations, $M'^{II}(\mu\text{-}CN)M^{III}$ and $M'^{III}(\mu\text{-}CN)M^{II}$ respectively, and a suitable perturbation matrix element exists to mix them together, the true ground state, Ψ_G, may be approximated as shown in equation (1), in which α is the ground-state

$$\Psi_G = (1 - \alpha^2)^{\frac{1}{2}}\psi_r + \alpha\psi_p \qquad (1)$$

delocalisation coefficient. The Hush formulae [equations (2)–(3), H_{rp} is the interaction energy and d is the intermetallic

$$H_{rp} = \nu_{max}\alpha = 2.05 \times 10^{-2}\left(\frac{\nu_{max}}{d}\right)\left(\frac{\varepsilon_{max}\Delta\nu_{\frac{1}{2}}}{\nu_{max}}\right)^{\frac{1}{2}} \qquad (2)$$

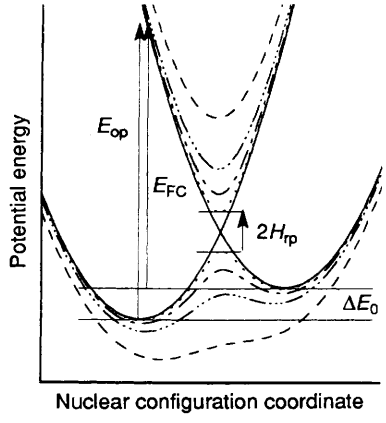

Fig. 1 Potential energy diagram for an asymmetric mixed-valence complex ($\Delta E_0 > 0$) as a function of nuclear configuration

$$\alpha^2 = 4.24 \times 10^{-4}\left(\frac{\varepsilon_{max}\Delta\nu_{\frac{1}{2}}}{\nu_{max}d^2}\right) \qquad (3)$$

distance][4] are applicable when $\alpha^2 \ll 1$, corresponding to the weak coupling limit described in the Robin–Day scheme as Class II. Fig. 1 illustrates the coupling between the potential energy surfaces and defines the relevant electronic parameters. The solid lines refer to the strictly localised wavefunctions ψ_r and ψ_p and the broken lines to the eigenstate states, for a number of different coupling strengths. The degree of electronic asymmetry, between ψ_r and ψ_p, is denoted by ΔE_0. The i.v.c.t. energy, ν_{max}, is represented by E_{op} which is related to ΔE_0 and the Franck–Condon barrier to electron transfer, E_{FC}, through equation (4), where χ_i and χ_o are the inner- and outer-sphere

$$E_{op} = \Delta E_0 + E_{FC} = \Delta E_0 + \chi_i + \chi_o \qquad (4)$$

reorganisational energies.[16]

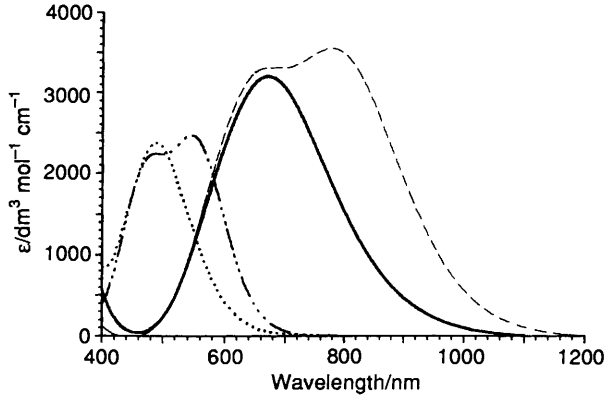

Fig. 2 Absorption spectra of complex **1** (——), **4** (– – –), **5** (· · ·) and **6** (— · · —) in acetonitrile showing the effect of metals upon the intervalence charge-transfer band

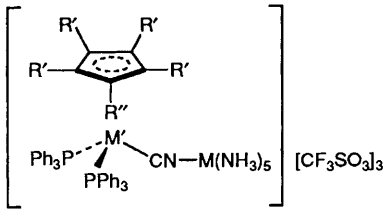

	M′	M	R′	R″
1	Ru	Ru	H	H
2	Ru	Ru	H	Me
3	Ru	Ru	Me	Me
4	Os	Ru	H	H
5	Ru	Os	H	H
6	Os	Os	H	H

Results and Discussion

Syntheses.—All the binuclear complexes described in this study, of general formula $[(\eta^5\text{-}C_5R_5)(PPh_3)_2M'(\mu\text{-}CN)M(NH_3)_5][CF_3SO_3]_3$ (M,M′ = Ru, Os; $C_5R_5 = C_5H_5$, C_5H_4Me or C_5Me_5), were synthesised by a simple coupling reaction, stirring a small excess of $[M'(\eta^5\text{-}C_5R_5)(PPh_3)_2(CN)]$ with $[M(NH_3)_5(OSO_2CF_3)][CF_3SO_3]_2$ in an acetone–dichloromethane mixture in the absence of light and oxygen overnight at 40 °C. Following extraction and recrystallisation, intensely coloured air-stable complexes were isolated and characterised by elemental analysis, IR and UV/VIS/NIR spectroscopies and cyclic voltammetry.

Electronic Absorption.—The mixed-valence compounds **1–6** are insoluble in water but soluble in a large number of organic solvents. Aerated solutions are stable for several hours but show a gradual weakening in intensity over a day or two, especially in strong sunlight.

There is little doubt that the intense colours of these complexes (Figs. 2 and 3) are due to intervalence charge-transfer transitions; none of the mononuclear precursors absorbs appreciably above 400 nm. Table 1 shows the intervalence charge-transfer characteristics for complexes **1–6** in selected solvents. Table 2 contains similar data for complex **2** in eighteen different aprotic solvents. To calculate [using equations (2) and (3)] the intervalence electronic coupling parameters from the absorption data, an intermetallic distance of 5.2 Å was used in all cases.

All the complexes (**1–6**) are of Class II nature. The absorption and coupling characteristics of complex **1**, for example, are typical for Class II species and similar to those of the well known[8] classical analogue $[(NC)_5Ru(\mu\text{-}CN)Ru(NH_3)_5]^-$ (aq) ($\varepsilon_{max} \approx 3000\,dm^3\,mol^{-1}\,cm^{-1}$, $\Delta\nu_{\frac{1}{2}} \approx 4500\,cm^{-1}$, $E_{op} = 685$ nm, $\alpha^2 \approx 1.5\%$, $H_{rp} \approx 1770\,cm^{-1}$).

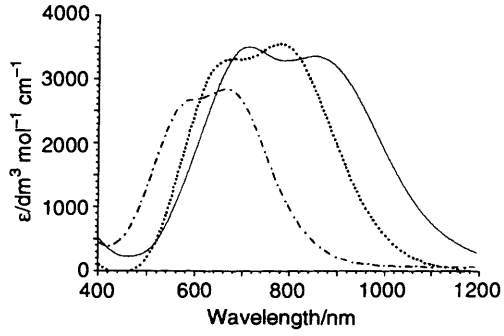

Fig. 3 Absorption spectra of complex **4** showing the effect of solvent, nitromethane (——), acetonitrile (· · ·) or dimethylacetamide (— · —), upon the spin-orbit component contributions to the intervalence charge-transfer band

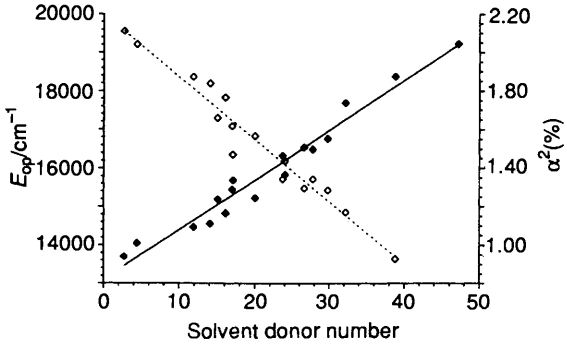

Fig. 4 Solvent effects upon the intervalence charge-transfer energy (E_{op}, ◆) and ground-state delocalisation coefficient (α^2, ◇) for complex **2** with linear regression fits

It is immediately obvious from Table 2 that the i.v.c.t. transition is strongly solvatochromic. Although Hush's treatment predicts[18] that E_{op} should be directly proportional to the solvent dielectric function, $(1/D_{op} - 1/D_s)$, this is not observed for any of the complexes **1–6**. Pronounced solvatochromic shifts also occur in the charge-transfer spectra of $[Ru(NH_3)_5(C_5H_4N)]^{2+/3+}$ complexes and originate from preferential stabilisation of the ammineruthenium(III) centre relative to the ruthenium(II) state through outer-sphere solvent–ammine metal hydrogen bonding.[19,20] Transition energies have been adequately correlated with the Gutmann[21] donor number (DN), or donicity, scale as well as with redox potentials.[19] For complex **2** over a large donicity range, the i.v.c.t. energy shifts by *ca.* 5500 cm^{-1} and linear regression analysis yields $E_{op} = 13\,116 + 128.9(DN)$ cm^{-1} with a correlation coefficient $R = 0.98$ (Fig. 4). This variation is similar to the value of 101 cm^{-1}/DN reported by Saleh and Crutchley[20] for a ligand-to-metal charge-transfer transition in a mononuclear penta-ammineruthenium complex, but is significantly smaller[8] than the 205 cm^{-1}/DN found for the i.v.c.t. transition in $[(OC)_5W(\mu\text{-}CN)Ru(NH_3)_5]^{2+}$. In terms of Fig. 1 increasing the solvent donicity primarily increases the extent of redox asymmetry, ΔE_0 (a relative vertical displacement of potential curves) and therefore increases E_{op} [equation (4)].

Table 2 also shows that the peak (and integrated) intensities as well as α^2 [$= 2.198 - 0.032(DN)\%$, $R = 0.98$] vary by a factor of two over the solvent range (Fig. 4). Although changes in $\Delta\nu_{\frac{1}{2}}$ and H_{rp} are small these also appear to show a correlation with donor number.

For comparable systems, the extent of vibrational excitation, E_{FC} [equation (4)], in the i.v.c.t. can be correlated with the bandwidth, and is expected to decrease as the difference between

Table 1 Intervalence charge-transfer data for the mixed-valence complexes **1**–**6** in selected solvents

Complex	Solvent[a]	E_{op}/nm (cm^{-1})	ε_{max}/dm^3 mol^{-1} cm^{-1}	$\Delta\nu_{\frac{1}{2}}$[b]/cm^{-1}	α^2 (%)	H_{rp}/cm^{-1}	f[c]
1	$MeNO_2$	716 (13 963)	3715	4980	2.08	2015	0.0851
	MeCN	671 (14 900)	3210	5000	1.69	1940	0.0738
	Me_2CO	633 (15 794)	3240	4980	1.60	1999	0.0740
	dma	590 (16 945)	2780	5080	1.31	1940	0.0650
2	MeCN	687 (14 552)	3250	5250	1.84	1973	0.0785
3	MeCN	773 (12 933)	3085	4880	1.83	1750	0.0693
4[d]	$MeNO_2$	851 (11 750)	3370	7070	3.18	2095	0.1096
		712 (14 040)	3515				
	PhCN	775 (12 900)	3375	7045	2.89	2195	0.1094
		656 (15 240)	3260				
	MeCN	776 (12 885)	3560	6470	2.80	2160	0.1060
	dma	662 (15 100)	2860	6850	2.03	2155	0.0901
5	$MeNO_2$	510 (19 600)	2620	5300	1.11	2070	0.0638
	MeCN	488 (20 485)	2380	5345	0.97	2020	0.0585
	dma	446 (22 415)	2320	5080[e]	0.82	2035	0.0542
6[d]	$MeNO_2$	576 (17 355)	2445	7165	1.58	2185	0.0806
		502 (19 915)	2530				
	MeCN	545 (18 345)	2475	6590	1.39	2165	0.0750
		485 (20 615)	2445				
	dma	493 (20 280)	2430	6870	1.29	2305	0.0768

[a] dma = *N*,*N*-Dimethylacetamide. [b] Estimated error of 100 cm^{-1}. [c] Oscillator strength. [d] The band profile (Fig. 3) exhibits two peak absorbances. [e] Calculated by doubling the low energy half bandwidth.

Table 2 Intervalence charge-transfer data for complex **2** in organic aprotic solvents

Solvent	DN[a]	E_{op}/nm (cm^{-1})	ε_{max}/dm^3 mol^{-1} cm^{-1}	$\Delta\nu_{\frac{1}{2}}$[b]/cm^{-1}	α^2 (%)	H_{rp}/cm^{-1}	f
Nitromethane	2.7	730[c] (13 695)	3650	5050	2.11	1990	0.0848
Nitrobenzene	4.4	712 (14 041)	3570	5120	2.04	2006	0.0841
Dimethyl sulfate	—	710 (14 080)	3470	5370	2.07	2030	0.0857
Benzonitrile	11.9	691 (14 468)	3395	5090	1.87	1980	0.0795
Acetonitrile	14.1	687 (14 552)	3250	5250	1.84	1973	0.0785
Propylene carbonate	15.1	658 (15 193)	3056	5265	1.66	1958	0.0740
Butyronitrile	16.1	674 (14 833)	3215	5200	1.77	1972	0.0769
Acetone	17.0	647 (15 452)	3010	5300	1.62	1966	0.0734
Ethyl acetate	17.1	637 (15 694)	2861	5152	1.47	1905	0.0678
Tetrahydrofuran	20.0	656 (15 240)	2930	5200	1.57	1908	0.0701
Tributyl phosphate	23.7	612 (16 335)	2660	5270	1.35	1895	0.0645
Formamide	24.0	631 (15 843)	2713	5357	1.44	1900	0.0669
N,*N*-Dimethylformamide	26.6	604 (16 552)	2550	5370	1.30	1885	0.0630
N,*N*-Dimethylacetamide	27.8	606 (16 497)	2644	5353	1.35	1913	0.0651
Dimethyl sulfoxide	29.8	596 (16 774)	2570	5360	1.29	1903	0.0634
N,*N*-Diethylacetamide	32.2	565 (17 694)	2360	5600	1.17	1915	0.0608
Hexamethylphosphoramide	38.8	544 (18 377)	1950	5590	0.93	1772	0.0501
Tris(*N*,*N*-tetramethylene)-phosphoramide	47.2[d]	520 (19 225)	—	—	—	—	—

[a] Solvent donor numbers from ref. 16. [b] Full bandwidth at half the maximum intensity; estimated error of 100 cm^{-1}. [c] Ultra pure nitromethane gives E_{op} = 737 ± 7 nm. [d] Ref. 17.

the ground state and excited state internuclear distances in both inner- and outer-co-ordination spheres becomes smaller.[20] The outer-sphere contribution (χ_o) to the bandwidth should increase with increasing donor number, because stronger hydrogen bonding interactions effectively increase the extent of reorganisation. Table 2 shows that the bandwidth does increase with donicity as expected, corresponding to small horizontal displacements of the potential surfaces in Fig. 1.

Correlations of linear regression data with solvent donor number for complex **2** yields several relationships. The effects of solvent upon E_{op} and α^2 (see above), for example, are shown in Fig. 4 and ε_{max} = 3815 − 45.6 (DN) dm^3 mol^{-1} cm^{-1} (R = 0.98) and f = 0.0887 − 0.0009 (DN) (R = 0.97). These trends can be qualitatively understood in terms of perturbation theory. The oscillator strength, f, is related to the dipole strength, D, which is in turn proportional to the total transition probability[22] [equation (5)]. For gaussian envelopes, equation (6)

$$f = 1.085 \times 10^{11} G\nu_{max} D \quad (5)$$

$$f \approx 4.6 \times 10^{-9} \varepsilon_{max} \Delta\nu_{\frac{1}{2}} \quad (6)$$

can be used[22] to calculate f. Comparing equations (3), (5) and (6), the function f/E_{op} is proportional to α^2. That is to say, the i.v.c.t. transition probability is directly proportional to the square of the mixing cofficient coupling the zero-order wavefunctions of the redox isomers together. An increase in solvent donicity increases the redox asymmetry, so that mixing of the basis states decreases as is shown by the values of α in Table 2.

A more interesting discussion concerns the interaction energy, H_{rp}. In a superexchange description[23] of bridge-mediated electron transfer, H_{rp} depends critically upon the energy separations between both the donor and acceptor metal

$$[(\eta^5\text{-}C_5H_4Me)(PPh_3)_2Ru^{II}(\mu\text{-}CN)Ru^{III}(NH_3)_5]^{3+} \begin{cases} \rightarrow [(\eta^5\text{-}C_5H_4Me)(PPh_3)_2Ru^{III}(\mu\text{-}CN^-)Ru^{III}(NH_3)_5]^{3+} & (7) \\ \rightarrow [(\eta^5\text{-}C_5H_4Me)(PPh_3)_2Ru^{II}(\mu\text{-}CN^+)Ru^{II}(NH_3)_5]^{3+} & (8) \end{cases}$$

orbitals and the orbitals of the bridge. The dominant charge-transfer pathways involving electron and hole transfer are represented, for complex **2**, by equations (7) and (8) respectively. Hupp[23] has shown that there is a strong solvent dependence of H_{rp} for the pyrazine (pyz)-bridged Class II mixed-valence compound $[(bipy)_2(Cl)Ru^{II}(\mu\text{-}pyz)Ru^{III}(NH_3)_4(py)]^{4+}$ (bipy = 2,2′-bipyridine, py = pyridine). He argues that available spectroscopic evidence indicates that there is a strong solvent dependence of the energy of the ligand-to-metal charge transfer (hole transfer) analogous to equation (8), which is a consequence of the association of donor solvents with the acidic ammine protons. On the other hand, the energy of the metal–ligand counterpart [equation (7)] is less perturbed by solvent donicity in the absence of acidic sites on the donor metal. The observed solvent dependence of H_{rp} in the pyrazine complex is therefore taken to mean that hole transfer is significant. Nevertheless the relatively low energy of the metal–ligand charge-transfer transitions indicates that electron transfer is still the dominant mechanism. In complex **2** the solvent sensitivity of H_{rp} is much smaller than in the pyrazine-bridged complex, suggesting that the hole-transfer process is relatively unimportant. We interpret this in terms of the larger π–π^* separation in the cyanide bridge which places the cyanide π orbital too low in energy to be a significant contributor to the hole-transfer mechanism.

A solution of complex **2** in a weakly donating solvent (*e.g.* nitromethane) is turquoise blue. Adding small amounts of tetrabutylammonium salts induces colour changes. Dihydrogenphosphate, nitrate or chloride anions immediately produce bright purple solutions, whereas the effect of iodide, bromide or hydrogensulfate anions, for example, is less evident; blue colours persist. This is clear evidence for the influence of anion association upon i.v.c.t. energies due to outer-sphere hydrogen bonds with the ammine groups in weakly donating solvents. An X-ray study may be interesting in this respect. Preferential binding of one component of a solvent mixture has been reported.[5,6] We note that an anion donicity scale, defined relative to the Gutmann solvent scale, has been described recently.[24]

The other complexes **1** and **3**–**6** show similar solvent effects to complex **2**, although quantitative solvent studies were not undertaken. The data shown in Table 1 illustrate a number of points.

For analogous mixed-valence compounds in the same solvents, the pentaammineosmium(III) complexes exhibit i.v.c.t. absorptions at significantly higher energies (*ca.* 5500 cm^{-1}), with reduced intensities (*ca.* 75%) and smaller delocalisation cofficients (*ca.* 50%), than the pentaammineruthenium(III) analogues (Fig. 2). These changes follow from the increased redox asymmetry in the ammineosmium complexes; the redox potentials of hexaammine-ruthenium(III) and -osmium(III) ions are reported to be +0.10 and −0.78 V [*vs.* normal hydrogen electrode (NHE)] respectively in aqueous solution.[25,26]

For a given solvent pair (*e.g.* acetonitrile and dimethylacetamide), differences in E_{op} (*ca.* 1900–2100 cm^{-1}) are essentially independent of the nature of the complex.

The i.v.c.t. bands of the cyclopentadienylosmium mixed-valence complexes **4** and **6** exhibit a pronounced splitting and an anomalously large bandwidth which is not observed in the cyclopentadienylruthenium bimetallics **1**–**3** and **5**. This effect can only be attributed to spin-orbit splitting in the osmium(III) low-spin d^5 excited state configuration.[27] An analogous spin-orbit coupling occurs for **1**–**3** and **5** but, because of the smaller coupling constants [$\zeta(Os^{III}) \approx 3000$ cm^{-1}, $\zeta(Ru^{III}) \approx 1250$ cm^{-1}],[28] the effect is not clearly observed. The low symmetry around the donor metal in these complexes should lead to three excited-state components, however, only two are clearly visible. There appears to be only one example[29] of a cyanide-bridged mixed-valence compound showing three components in the near-infrared region.

The solvent effect on the relative intensities of the spin-orbit components is of particular interest. For both cyclopentadienylosmium complexes **4** and **6**, the highest intensity component is highest in energy in nitromethane (and nitrobenzene) solutions, but in more strongly donating solvents the order is reversed (Fig. 3). Such effects have not, to our knowledge, been reported. Their origin is not clear at present but further experiments may be worthwhile.

Although the identity of each metal ion strongly influences the i.v.c.t. characteristics, the effect of methyl substitution on the cyclopentadienyl ring affects E_{op} to a much smaller degree. In the series **1**–**3**, the shift appears to be proportional to the number of methyl groups with $\delta(E_{op}) \approx -400$ cm^{-1} per methyl substituent. The other mixed-valence properties, intensity, bandwidth and coupling parameters, do not vary significantly with the extent of methylation.

Cyclic Voltammetry.—Tables 3 and 4 show the oxidative, E_{pa}, and reductive, E_{pc}, half-wave potentials (if resolved) and redox potentials, $E_{\frac{1}{2}} = \frac{1}{2}(E_{pa} + E_{pc})$, for both the monometallic cyclopentadienyl precursors in acetonitrile and their associated pentaamminemetal mixed-valence compounds. The measurements for each mixed-valence compound were made in acetonitrile so that any ammine deficiency, which could have occurred through overheating in the preparation of the triflate precursor, could be detected by the appearance of a high potential wave typical of nitrile-substituted ammines; for example $E_{\frac{1}{2}}$ for $[Ru(NH_3)_5(NCMe)]^{2+/3+}$ is +0.43 V (*vs.* NHE).[25] In complexes **1**–**6** no such evidence was observed. In some cases electrochemical data are also given in nitromethane and acetone solutions. Figs. 5 and 6 show some typical voltammograms of the monometallic cyanides (dotted traces) and their associated mixed-valence compounds with pentaammineruthenium(III) (solid lines) or pentaammineosmium(III) (dash–dot traces).

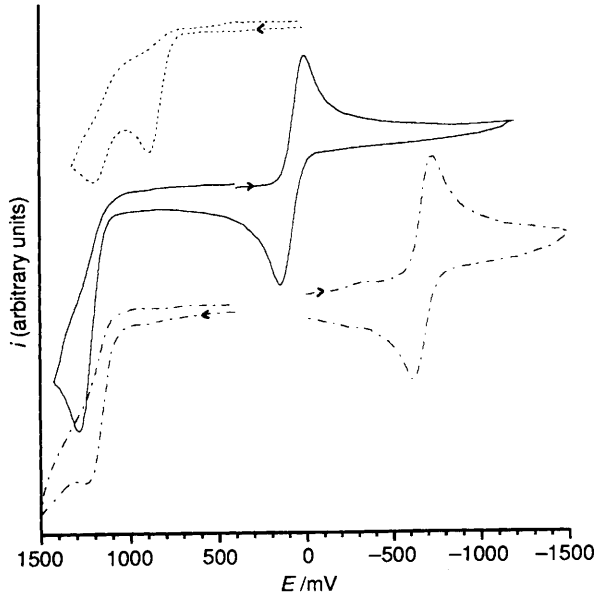

Fig. 5 Cyclic voltammograms for $[Ru(\eta^5\text{-}C_5H_5)(PPh_3)_2(CN)]$ (· · ·) and its associated mixed-valence complexes with pentaamine-ruthenium(III) (**1**, ——) and -osmium(III) (**5**, — · —) in acetonitrile at 100 mV s^{-1}

Table 3 Electrochemical data for complexes **1–6**[a]

		$(\eta^5\text{-}C_5R_5)M'(PPh_3)_2(\mu\text{-}CN)$–			–$M(NH_3)_5$		
Complex	Solvent	E_{pa}/V	E_{pc}/V	$E_{\frac{1}{2}}$/V	E_{pa}/V	E_{pc}/V	$E_{\frac{1}{2}}$/V
1	MeCN	+1.27	*b*	*b*	+0.145	+0.01	+0.08
2	MeCN	+1.24	*b*	*b*	+0.14	+0.05	+0.095
	$MeNO_2$	+1.20	+1.12	+1.16	+0.235	+0.155	+0.195
	Me_2CO	+1.235	+1.15	+1.19	+0.095	+0.005	+0.05
	Me_2SO	*b*	*b*	*b*	−0.135	−0.22	−0.175
3	MeCN	*ca.* +1.2	*b*	*b*	+0.215	+0.11	+0.17
	Me_2CO	+1.165	+1.025	+1.095	+0.19	+0.06	+0.125
4	MeCN	+1.27	*b*	*b*	+0.14	−0.01	+0.065
	$MeNO_2$	+1.235	+1.135	+1.185	+0.16	+0.07	+0.115
	Me_2CO	+1.27	+1.16	+1.215	+0.08	−0.06	+0.01
5	MeCN	+1.25	*b*	*b*	−0.615	−0.73	−0.67
6	MeCN	+1.08	+0.94[c]	+1.01	−0.60	−0.78	−0.69

[a] Potentials [±0.01 V; *vs.* saturated calomel electrode (SCE)] at 100 mV s^{-1}; $E_{\frac{1}{2}} = \frac{1}{2}(E_{pa} + E_{pc})$. Under similar conditions for ferrocene, E_{pa} = +0.48, E_{pc} = +0.35 and $E_{\frac{1}{2}}$ = +0.415 V in acetonitrile; $E_{\frac{1}{2}}$ = +0.52 and +0.4 V in acetone and nitromethane, respectively. [b] Potentials not resolved. [c] At 200 mV s^{-1}.

Table 4 Electrochemical data for $[M'(\eta^5\text{-}C_5R'_4R'')(PPh_3)_2(CN)]$*

Complex	Solvent	E_{pa}/ V	E_{pc}/ V	$E_{\frac{1}{2}}$/ V
$[Ru(\eta^5\text{-}C_5H_5)(PPh_3)_2(CN)]$	MeCN	+0.88	*b*	*b*
	$MeNO_2$	+0.90	+0.82	+0.86
$[Ru(\eta^5\text{-}C_5H_4Me)(PPh_3)_2(CN)]$	MeCN	+0.82	*b*	*b*
$[Ru(\eta^5\text{-}C_5Me_5)(PPh_3)_2(CN)]$	MeCN	+0.60	+0.53	+0.57
	$MeNO_2$	+0.60	+0.51	+0.55
$[Os(\eta^5\text{-}C_5H_5)(PPh_3)_2(CN)]$	MeCN	+0.80	+0.73	+0.765
	$MeNO_2$	+0.835	+0.73	+0.78

* See footnotes to Table 3 and ref. 30.

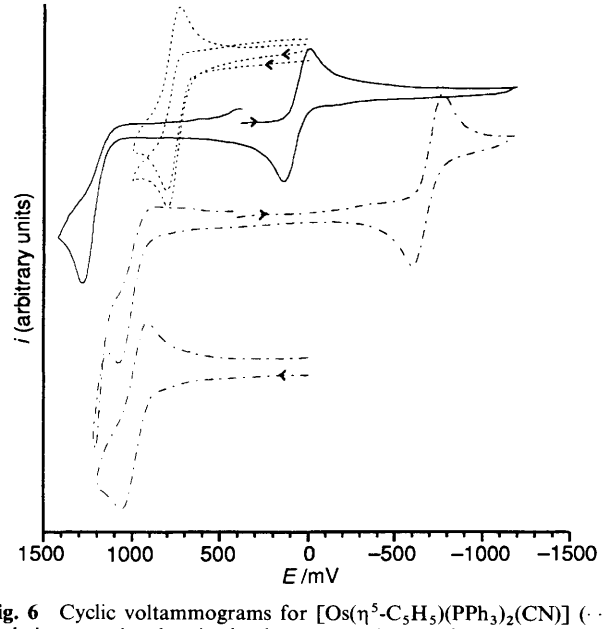

Fig. 6 Cyclic voltammograms for $[Os(\eta^5\text{-}C_5H_5)(PPh_3)_2(CN)]$ (· · ·) and its associated mixed-valence complexes with pentaammineruthenium(III) (**4**, ——) and -osmium(III) (**6**, — · —) in acetonitrile at 100 mV s^{-1} and additionally at 200 mV s^{-1} for the bottom voltammogram for complex **6**

The electrochemistry of the cyclopentadienylmetal precursor complexes in acetonitrile is described elsewhere.[30] The redox waves between +0.7 and +1.0 V correspond to irreversible M^{II}–M^{III} oxidation. By analogy therefore, the irreversible couples near +1.2 V in complexes **1–6** are similarly assigned. The near-reversible couples around 0.0 V are assigned to M^{III}–M^{II} reduction at the pentaammineruthenium centre and those near −0.7 V to a similar process at the pentaammineosmium centre. In general the ammine centres exhibit current peak ratios (i_{pa}/i_{pc}) close to unity and follow the Randles–Sevcik relation ($i_p/v^{\frac{1}{2}}$ = constant) for scan rates, v, between 50 and 600 mV s^{-1}. The separation of the half-wave peak potentials (ΔE_p), however, are greater than the Nernstian value of 59 mV, varying typically from *ca.* 200 mV at 600 mV s^{-1} to *ca.* 110 mV at 50 mV s^{-1}. Under the same conditions, the reversible ferrocene couple exhibits ΔE_p = 130 mV at 100 mV s^{-1}, implying that solution resistance effects are responsible.

The two cyclopentadienylosmium complexes **4** and **6** are particularly interesting. The electrochemical reversibility and potential of the cyclopentadienylosmium centres in acetonitrile appear to depend critically upon the nature of the amminemetal centre and the extent of valence delocalisation in the ground state. At scan rates greater than 50 mV s^{-1} the oxidative and reductive half-wave current peaks in $[Os(\eta^5\text{-}C_5H_5)(PPh_3)_2(CN)]$ are resolved (Fig. 6, dotted traces). In complex **4**, however, the reductive half-couple peak (E_{pc}) of the cyclopentadienylosmium centre is absent at scan rates up to 400 mV s^{-1}, whereas in complex **6** it is revealed with scan rates of 200 mV s^{-1} and greater (Fig. 6). By way of comparison, in the $[Ru(\eta^5\text{-}C_5H_5)(PPh_3)_2(CN)]$ based complexes **1** and **5** (Fig. 5), the analogous peaks in the reductive current are never observed in acetonitrile. In acetone and nitromethane solutions, however, these half-waves are observed, albeit with relatively small peak currents, for all mono- and bi-nuclear complexes at 100 mV s^{-1}. These results are consistent with the co-ordinating ability of acetonitrile which traps unstable electrochemical oxidation products irreversibly. We particularly note the small reduction waves around +0.4 V (in **4**) (Fig. 6) which are only observed in scans incorporating redox processes at both metal centres. We have reported similar but more pronounced effects elsewhere[8] for related mixed-valence compounds. The effect of the solvent on the redox reversibility of the cyclopentadienylmetal centre is the most striking for complex **3**; Fig. 7 shows the voltammograms in acetone and acetonitrile.

Electrochemical studies in different solvents show that although the cyclopentadienylmetal redox potentials only vary slightly, the amminemetal centre potentials are strongly solvent dependent. The pentaammineruthenium reduction potentials for complex **2** in nitromethane, acetonitrile and dimethyl sulfoxide are +0.195, +0.095 and −0.175 V (*vs.* SCE) respectively. Such evidence merely confirms the expectation that outer-sphere solvent–ammine hydrogen bonding alters the degree of redox asymmetry and therefore the i.v.c.t. parameters as discussed in the previous section. Preliminary studies reveal that using nitromethane, nitrobenzene and acetone solvents

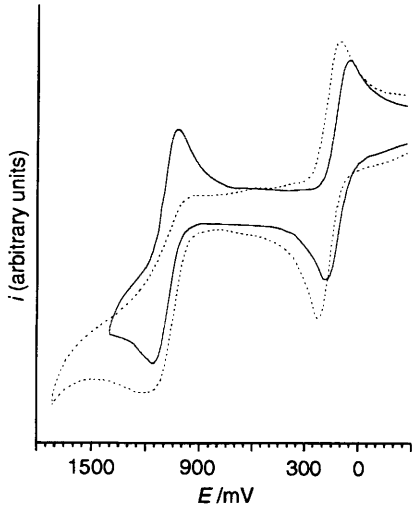

Fig. 7 Cyclic voltammograms for complex **3** in acetone (——) and acetonitrile (· · ·) showing the effect of solvent upon the reversibility of the cyclopentadienylmetal centre

enables accurate redox potentials to be measured for both metal centres in complex **2** whereas in nitrile and amide solvents the reductive half-wave of the organometallic centre is always absent. In tetrahydrofuran and tributyl phosphate the pentaamminemetal centre shows very broad overpotentials, presumably because of the low dielectric constants of these solvents.

The relationship between the i.v.c.t. energies, donor number and the electrochemical results is usually discussed in relation to a thermodynamic cycle.[31] It can be shown that the solvent effect upon the difference between the donor and acceptor metal redox potentials, $\Delta E_{\frac{1}{2}}$, corrected using the ferrocene assumption,[32] correlates with changes in ΔE_0, E_{op} and therefore with donor number. A plot of E_{op} against $\Delta E_{\frac{1}{2}}$ should give a straight line with a gradient of one, deviations from which can give information on the details of mixed-valence redox thermodynamics.[31,33,34] It is unfortunate that for complex **2** few solvents give sufficient redox reversibility for accurate values of $\Delta E_{\frac{1}{2}}$ to be used in such correlations. The poor resolution of the irreversible cyclopentadienylmetal redox potentials is troublesome. However, preliminary electrochemical studies on a related cyclopentadienyliron pentaammineruthenium mixed-valence complex reveal quasi-reversible redox behaviour for both metal centres in many solvents.[12]

Values of $\Delta E_{\frac{1}{2}}$ can also be used to calculate comproportionation stability constants[35] which for complexes **1–6** are typically $> 10^{16}$, a result mainly due to substantial redox asymmetry rather than to delocalisation.

Infrared Spectroscopy.—Infrared data (KBr pellet) for the monometallic precursors and their associated complexes **1–6** are shown in Table 5. The spectra of the mixed-valence compounds show characteristics of both metallic fragments but the main effect of binuclear complex formation is a large shift to lower frequency of the cyanide stretch, ν(CN). The electron-rich metal(II) centres are coupled to the pentaamminemetal(III) centres which are known to be strong π acceptors. Bignozzi *et al.*[36] have recently discussed electronic effects on the stretching frequencies in both bridging and terminal cyanide ligands. Kinematic coupling, a mechanical constraint upon C≡N motion imposed by the second metal, shifts ν(CN) to higher frequency. Back-bonding from the carbon-bound metal into the C≡N bond is expected to increase on bridge formation, due to withdrawal of charge from the nitrogen to the second metal. This leads to a decrease in ν(CN) but is dependent upon the π-accepting nature of other competing ligands. Back-bonding from the nitrogen-bound metal is not important in complexes **1–6**.

Table 5 Infrared transmittance data in the cyanide region for complexes **1–6**

Complex	ν(CN)[a]/cm^{-1}	$\Delta\nu_{\frac{1}{2}}$[b]/cm^{-1}	Medium
1	2011 (2079)	60	KBr
1	2004 (2072)	48	$MeNO_2$
1	2007	65	MeCN
1	2013	101	Tributyl phosphate
1	2017	150	Diethylacetamide
1[c]	2090	—	$MeNO_2$
2	2003 (2072)	63	KBr
3	1981 (2066)	37	KBr
4	2011 (2065)	37	KBr
5	2050 (2079)	22	KBr
5	2038 (2072)	22	$MeNO_2$
6	2038 (2065)	27	KBr

[a] Bracketed figures refer to the monometallic precursor complexes. [b] Bandwidth at half the maximum absorption relative to the baseline absorption. [c] After reduction by Zn(Hg) or electrochemically (at −0.5 V *vs.* SCE).

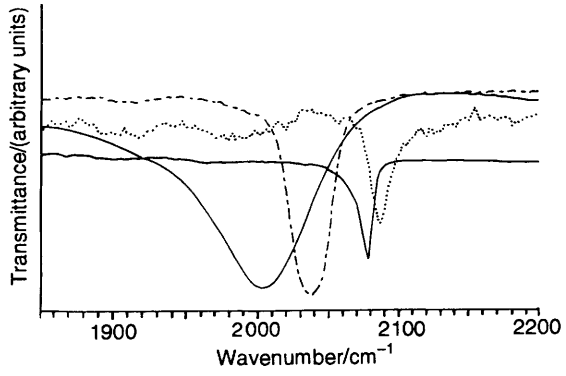

Fig. 8 Infrared transmittance spectra in the cyanide region for [Ru(η^5-C_5H_5)$(PPh_3)_2$(CN)] (KBr, ——) and its associated mixed-valence complexes with pentaammine-ruthenium(III) (**1**, – – –) and -osmium(III) (**5**, — · —) and complex **1** after reduction (· · ·) in nitromethane

In Fig. 8 the infrared spectra in the cyanide region of the cyclopentadienylruthenium precursor (KBr) and its metallated derivatives, in nitromethane solution, illustrate the influence of the amminemetal and its oxidation state upon ν(CN). Several points are noteworthy. The mixed-valence forms, **1** and **5**, show ν(CN) at a lower frequency than the monometallic precursor on account of the strong π-accepting nature of the pentaammine-metal(III) moiety. The greater shift exhibited by complex **1**, −68 cm^{-1}, compared to −29 cm^{-1} for complex **5** is consistent with the greater mixing coefficient (α^2) in the former (Table 1).

The pentaammineruthenium mixed-valence complexes are unique in displaying an exceptionally broad asymmetric-bridging cyanide absorption. This cannot be attributed to sample inhomogeneity because the homovalent reduced form exhibits a narrow bandwidth comparable to that of the monometallic precursor.

The homovalent form of complex **1** was prepared by zinc amalgam, electrochemical and hydrazine reduction methods in nitromethane under nitrogen but not isolated. Although other workers[36] have used hydrazine to manipulate the oxidation state of pentaammineruthenium centres, we found it to give anomalous results. Whilst zinc and electrochemical reductions gave identical results showing the bridging cyanide absorption at 2090 cm^{-1} for the reduced form of complex **1**, hydrazine reduction initially yielded a peak at 2090 cm^{-1} which was completely replaced by a peak at 2110 cm^{-1} within a few minutes. This suggests that hydrazine may react with and not simply reduce complex **1**. The shift to higher frequency, 2090 cm^{-1}, upon reduction is expected given that pentaammine-

ruthenium(II) is not a π-acceptor; ν(CN) is then dominated by the kinematic effect.

The bridging cyanide frequencies of complexes **1–6** in nitromethane solutions are consistently lower (10–15 cm^{-1}) than those recorded in polycrystalline KBr pellets, emphasising the sensitivity of this mode to the molecular environment. Considering that the redox properties of the amminemetal centres can be tuned over a large range through the choice of medium, the solvent effect upon the infrared frequency of the bridging cyanide was investigated. Solvents were selected according to their transparency in the cyanide window 1700–2300 cm^{-1} and to cover a range of donicity. Table 5 shows the results in the solvents nitromethane, acetonitrile, tributyl phosphate and diethylacetamide.

Although the accuracy of the ν(CN) values is poor due to the large bandwidths the trends appear unequivocable; the broadness and frequency increase with solvent donicity. The trend in frequency is understood in similar terms to the differences between complex **1** and **5**. Increasing donicity decreases the reduction potential of the ammineruthenium centre. The reduction of the acceptor properties of the ruthenium(III) centre is then reflected in less back-bonding from the donor metal to the cyanide.

Conclusion

The facile synthesis of the bimetallic complexes **1–6** composed of organometallic donors and Werner-co-ordinated acceptors augments the choice of discrete Robin–Day Class II mixed-valence complexes for associated studies. Complexes **1–6** are soluble in a wide range of aprotic organic solvents. Hydrogen bonding between the solvent and ammine centre provides a convenient method for tuning the intervalence charge transfer absorptions to an appropriate region of the UV/VIS spectrum whilst maintaining the localised charge distribution. We note that such effects are particularly useful in experiments for determining molecular non-linear optic coefficients where residual absorption at laser wavelengths can be troublesome and resonance enhancement is important. Solvent effects upon the i.v.c.t. characteristics of **1–6** can be rationalised by reference to the Gutmann solvent donor number scale. Complexes **4** and **6** show an interesting spin-orbit splitting in the i.v.c.t. band, the relative intensities of the components being solvent dependent.

Experimental

Infrared spectra were recorded on a Mattson Polaris FTIR instrument as KBr pellets with 4 cm^{-1} resolution. Solution infrared studies were undertaken with a KBr plate solution cell with a path length of 0.2 or 0.5 mm. Pure solvent spectra were subtracted from sample spectra by computer. Electronic absorption spectra were recorded on a Perkin-Elmer 552 or a Lambda 9 spectrometer with appropriate computerised data acquisition. AnalaR grade solvents were routinely dried through contact with activated molecular sieves (Linde 4 Å) and often passed over activated neutral alumina immediately prior to use. Tetrahydrofuran was distilled from sodium. Acetonitrile was used as supplied (HPLC, 99.9%) or distilled from CaH_2. Electrochemistry was performed on a Princeton Applied Research potentiostat (model 273) with a conventional three-armed cell using a standard saturated KCl(aq) calomel reference electrode, platinum-bead working and platinum-wire counter electrodes in dry organic solvents with tetrabutylammonium tetrafluoroborate (0.2 g in 10 cm^3) as the base electrolyte. Voltammograms were recorded under nitrogen (or argon) at scan rates of 100, 200 or 400 mV s^{-1} with typical peak currents of the order 10–50 μA. It proved necessary to clean the platinum electrodes and the reference electrode frit after each scan.

The complexes, $[M(NH_3)_5(OSO_2CF_3)][CF_3SO_3]_2$ (M = Ru or Os)[37,38] and all the cyclopentadienylmetal cyano precursors[30] were prepared by literature methods. The mixed-valence complexes $[(\eta^5\text{-}C_5R_5)(PPh_3)_2M'^{II}(\mu\text{-}CN)M^{III}(NH_3)_5][CF_3SO_3]_3$ **1–6** were all prepared following the method for complex **1**.

Synthesis of $[(\eta^5\text{-}C_5H_5)(PPh_3)_2Ru(\mu\text{-}CN)Ru(NH_3)_5][CF_3SO_3]_3$ **1**.—A sample of $[Ru(\eta^5\text{-}C_5H_5)(PPh_3)_2(CN)]$ (0.4 g, 0.5 mmol) was dissolved in dichloromethane (3 cm^3) and acetone (40 cm^3) was added. The solution was deaerated and $[Ru(NH_3)_5(OSO_2CF_3)][CF_3SO_3]_2$ (0.24 g, 0.38 mmol) added. The solution rapidly turned blue and was heated overnight, with stirring, at 40 °C under an inert atmosphere. The following work-up was carried out in the air. The blue solution was evaporated to dryness under reduced pressure and low temperature (< 40 °C) and was taken up in chloroform (75 cm^3) or dichloromethane. A blue precipitate readily formed upon the addition of excess diethyl ether. The solid was filtered using a glass sinter (no. 3), washed with toluene and diethyl ether and slowly extracted through the sinter with chloroform or dichloromethane. The solution was evaporated to a small volume (*ca.* 15 cm^3) and the product precipitated by the slow addition of excess diethyl ether. The blue microcrystals were filtered, washed with diethyl ether and vacuum dried. Yields 60–80% [Found (calc.): C, 40.0 (40.0); H, 3.7 (3.7); N 6.0 (6.2)%].

$[(\eta^5\text{-}C_5H_4Me)(PPh_3)_2Ru(\mu\text{-}CN)Ru(NH_3)_5][CF_3SO_3]_3$ **2**. Found (calc.): C, 39.4 (40.5); H, 3.7 (3.8); N, 6.0 (6.2)%.

$[(\eta^5\text{-}C_5Me_5)(PPh_3)_2Ru(\mu\text{-}CN)Ru(NH_3)_5][CF_3SO_3]_3$ **3**. Found (calc.): C, 41.8 (42.3); H, 4.4 (4.3); N, 5.5 (5.9)%.

$[(\eta^5\text{-}C_5H_5)(PPh_3)_2Os(\mu\text{-}CN)Ru(NH_3)_5][CF_3SO_3]_3$ **4**. Found (calc.): C, 37.5 (37.6); H, 3.5 (3.5); N, 5.5 (5.8)%.

$[(\eta^5\text{-}C_5H_5)(PPh_3)_2Ru(\mu\text{-}CN)Os(NH_3)_5][CF_3SO_3]_3$ **5**. Found (calc.): C, 37.9 (37.6); H, 3.6 (3.5); N, 5.7 (5.8)%.

$[(\eta^5\text{-}C_5H_5)(PPh_3)_2Os(\mu\text{-}CN)Os(NH_3)_5][CF_3SO_3]_3$ **6**. Found (calc.); C, 35.3 (35.4); H, 3.4 (3.3); N, 5.3 (5.5)%.

Acknowledgements

We are grateful to the SERC for support (to W. M. L.), Dr. P. D. Beer and Professor H. A. O. Hill for the use of electrochemical apparatus and the Clarendon laboratory for near-infrared absorption facilities.

References

1 *Mixed-Valence Compounds*, ed. D. B. Brown, NATO ASI, D. Reidel, Dordrecht, 1980, vol. 58C.
2 *Mixed-Valency Systems: Applications in Chemistry, Physics and Biology*, ed. K. Prassides, NATO, ASI, Kluwer, Dordrecht, 1991, vol. 343C.
3 C. Creutz, T. J. Meyer, A. Haim and N. S. Sutin, *Prog. Inorg. Chem.*, 1983, **28**, 1.
4 C. Creutz, *Prog. Inorg. Chem.*, 1983, **28**, 1.
5 J. A. Roberts, J. C. Bebel, M. L. Absi and J. T. Hupp, *J. Am. Chem. Soc.*, 1992, **114**, 7957.
6 J. C. Curtis, J. A. Roberts, R. L. Blackbourn, Y. Dong, M. Massum, C. S. Johnson and J. T. Hupp, *Inorg. Chem.*, 1991, **30**, 3856 and refs. therein.
7 M. B. Robin and P. Day, *Adv. Inorg. Chem. Radiochem.*, 1967, **10**, 247.
8 W. M. Laidlaw and R. G. Denning, *Polyhedron*, in the press.
9 W. M. Laidlaw and R. G. Denning, *Polyhedron*, in the press.
10 W. M. Laidlaw, R. G. Denning, T. Verbiest, E. Chauchard and A. Persoons, *Nature*, 1993, **363**, 58.
11 W. M. Laidlaw, R. G. Denning, T. Verbiest, E. Chauchard and A. Persoons, in *Organic, Metallo-organic and Polymeric Materials for Nonlinear Optical Applications, Proc. SPIE*, eds. S. R. Marder and J. W. Perry, 1994, **2143**, 14.
12 W. M. Laidlaw and R. G. Denning, unpublished work.
13 F. L. Atkinson, A. Christofides, N. G. Connelly, H. J. Lawson, A. C. Lyons, A. G. Orpen, G. M. Rosais and G. H. Worth, *J. Chem. Soc., Dalton Trans.*, 1993, 1441 and refs. therein; G. Barrado, G. A. Carriedo, C. D-Valenzuela and V. Riera, *Inorg. Chem.*, 1991, **30**, 4416.
14 Y. Dong and J. T. Hupp, *Inorg. Chem.*, 1992, **31**, 3170 and refs. therein.
15 N. S. Hush, *Prog. Inorg. Chem.*, 1967, **8**, 391.
16 Y. Marcus, *Chem. Soc. Rev.*, 1993, **22**, 409.

17 Y. Ozari and J. Jagur-Grodzinski, *J. Chem. Soc., Chem. Commun.*, 1974, 295.
18 B. P. Sullivan, J. C. Curtis, E. M. Kober and T. J. Meyer, *Nouv. J. Chim.*, 1980, **4**, 643.
19 J. C. Curtis, B. P. Sullivan and T. J. Meyer, *Inorg. Chem.*, 1983, **22**, 224.
20 A. A. Saleh and R. J. Crutchley, *Inorg. Chem.*, 1990, **29**, 2132.
21 V. Gutmann, *Electrochim. Acta*, 1976, **21**, 661.
22 A. B. P. Lever, *Inorganic Electronic Spectroscopy*, Elsevier, Amsterdam, 2nd edn., 1985.
23 J. T. Hupp, *J. Am. Chem. Soc.*, 1990, **112**, 1563.
24 W. Linert, R. F. Jameson and A. Taha, *J. Chem. Soc., Dalton Trans.*, 1993, 3181.
25 T. Matsubara and P. C. Ford, *Inorg. Chem.*, 1976, **15**, 1107.
26 P. A. Lay, R. H. Magnuson and H. Taube, *Inorg. Synth.*, 1986, **24**, 269.
27 W. M. Laidlaw and R. G. Denning, *Inorg. Chim. Acta*, 1994, **219**, 121.
28 B. N. Figgis, *Introduction to Ligand Fields*, Wiley-Interscience, New York, 1966.
29 J. R. Schoonover, C. J. Timpson, T. J. Meyer and C. A. Bignozzi, *Inorg. Chem.*, 1992, **31**, 3185.
30 W. M. Laidlaw and R. G. Denning, *J. Organomet. Chem.*, 1993, **463**, 199.
31 J. P. Chang, E. Y. Fung and J. C. Curtis, *Inorg. Chem.*, 1986, **25**, 4233.
32 J. T. Hupp, *Inorg. Chem.*, 1990, **29**, 5010.
33 K. S. Ennix, P. T. McMahon, R. de la Rosa and J. C. Curtis, *Inorg. Chem.*, 1987, **26**, 2660.
34 J. C. Curtis, R. L. Blackbourn, K. S. Ennix, S. Hu, J. A. Roberts and J. T. Hupp, *Inorg. Chem.*, 1989, **28**, 3791.
35 W. Kaim and V. Kasack, *Inorg. Chem.*, 1990, **29**, 4696.
36 C. A. Bignozzi, R. Argazzi, J. R. Schoonover, K. C. Gordon, R. B. Dyer and F. Scandola, *Inorg. Chem.*, 1992, **31**, 5260.
37 G. A. Lawrence, P. A. Lay, A. M. Sargeson and H. Taube, *Inorg. Synth.*, 1986, **24**, 257.
38 P. A. Lay, R. H. Magnuson and H. Taube, *Inorg. Chem.*, 1989, **28**, 3001.

Received 17*th February* 1994; *Paper* 4/00974F